

Improved Modeling of Pneumatic Muscle Actuator Using Recurrent Neural Network

Alexander Hošovský, Jana Mižáková, Ján Pitel

Department of Mathematics, Informatics and Cybernetics
Technical University of Kosice
Košice, Slovakia

alexander.hosovsky@tuke.sk, jana.mizakova@tuke.sk, jan.pitel@tuke.sk

Abstract—Derivation of models of complex nonlinear systems usually incorporates a number of simplifications in modeled phenomena with the level of these simplifications being dictated primarily by its intended purpose. If the overall model accuracy is insufficient, it might be helpful to use the powerful approximation capabilities of universal approximators like neural networks which are capable of approximating certain types of functions to arbitrary degree of accuracy. On the other hand, using black-box modeling techniques can impair the resulting extrapolation qualities of the model as well as eliminate its physical interpretation. Here an improved dynamic modeling of one-DOF pneumatic muscle actuator using recurrent neural network is proposed. The proposed method preserves the physical meaning of the model while improving its accuracy compared to the original analytic model. System and model responses are compared in closed-loop (using conventional PD controller) and all unmodeled dynamics is treated as disturbance which is identified using Elman neural network. It is shown that the resulting model is applicable for model-based control system design with greater precision.

Keywords—pneumatic actuator, recurrent neural network, disturbance, structural dynamics, PD controller

I. INTRODUCTION

Pneumatic artificial muscles (PAM) can be considered a class of special actuators with elastic construction and specific characteristics that make them distinctive from traditional actuators. Due to their light and compliant nature they are suitable for biomedical applications where contact with patients is of high importance [1]–[3]. Their use in industrial applications where the systems based on this type of actuator could possibly be used as an alternative to costly and human-unfriendly industrial robots (for special tasks where lower precision would be acceptable) was also proposed [4]–[6]. When a control for a PAM-based system is designed, it is advantageous to have a model of such a system so that its performance under various conditions can be predicted. Some basic properties and approaches useful for modeling PAMs and systems based on them were described in [7]–[11]. Rather detailed dynamic modeling of PAM including braid effects on contractile range and friction modeling can be found in works [12], [13]. In [14] the development of analytical dynamic model of PAM (FESTO MAS-20) using quick-release experiment can be found. Different approach with fuzzy logic

used for developing a dynamic predictive model was taken in [15]. In [16] a modified Hill's muscle model was used for deriving a dynamic model of Fluidic muscle for resistive training device.

Most of these works concentrate on development of analytical model of PAM. Such a model preserves physical interpretation of all variables and allows for better evaluation of the PAM-based system properties. On the other hand, PAM-based systems feature a number of complex phenomena which are difficult to model precisely and are well-suited for application of universal approximators (like neural networks and fuzzy systems). Hence it is proposed here to use basically an analytical model of PAM-based actuator with one rotational joint and use a complementary neural model for identification of disturbance term incorporating unmodeled effects.

II. USED METHODS

A. Dynamic Model of Pneumatic Muscle Actuator

The dynamic model of the used muscle actuator was derived in [17]–[19] using the results of our own research and experiments and some general principles presented in the works of other researchers. The model was derived for an actuator with one rotational axis driven by a pair of FESTO MAS-20 pneumatic muscles moving in a horizontal plane. From the physical point of view, the actuator model represents a multi-domain model with three distinctive physical domain parts: electrical, mechanical and pneumatic (Fig. 1).

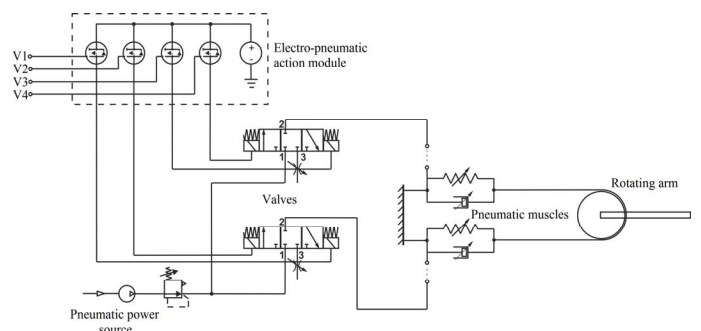


Fig. 1. Multi-domain physical representation of the pneumatic muscle actuator

To develop a dynamic model of the system, only pneumatic (valves) and mechanical parts (muscles and rotational axis) were taken into account. It can be observed from Fig.1 that the muscles are represented as parallel connection of nonlinear spring and nonlinear damper. This representation corresponds to a phenomenological model approach presented in [16]. The dynamics of pneumatic muscle can be described using the following nonlinear differential equation (in accordance with Newton's second law) [14]:

$$\ddot{\xi} = (1/m)[F_E - F_{nd}(\dot{\chi}, P_m) - F_{ns}(\chi, P_m)] \quad (1)$$

where ξ is muscle displacement [m], m is moved mass [kg], F_E is external force [N], F_{nd} is nonlinear damper force [N], F_{ns} is nonlinear spring force [N], χ is muscle contraction [-], P_m is absolute muscle pressure [Pa].

The nonlinear spring force term in (1) is a function of two variables (contraction and muscle pressure) which was approximated using fifth-order polynomial according to data available in manufacturer's specifications (Fig. 2). The second nonlinear term in (1) was a function of contraction speed $\dot{\chi}$ and muscle pressure P_m [14]:

$$F_{nd}(\dot{\chi}, P_m) = R\dot{\chi}P_m \quad (2)$$

where R is damping coefficient [$\text{m}^2\cdot\text{s}$], $\dot{\chi}$ is contraction speed [s^{-1}] and P_m is muscle pressure [Pa].

The pneumatic part is described using a differential equation for muscle pressure:

$$\dot{P}_m = P_{atm} \frac{\dot{V}_{atm}}{V_m} - P_m \frac{\dot{V}_m}{V_m} \quad (3)$$

where P_{atm} is atmospheric pressure [Pa], \dot{V}_{atm} is volume air flow through the valves [$\text{m}^3\cdot\text{s}^{-1}$], V_m is muscle volume [m^3] and \dot{V}_m is rate of muscle volume [$\text{m}^3\cdot\text{s}^{-1}$].

The term for muscle volume was approximated using third-order polynomial in the following form (including the rate of change of muscle volume):

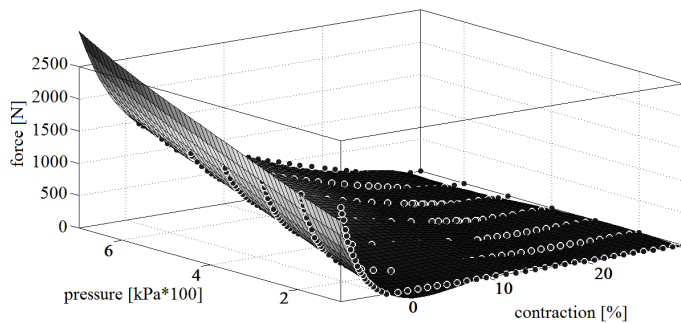


Fig. 2. Approximation of nonlinear spring force term in muscle dynamics equation

$$\begin{aligned} V_m &= a\chi^3 + b\chi^2 + c\chi + d \\ \dot{V}_m &= 3a\chi^2\dot{\chi} + 2b\chi\dot{\chi} + c\dot{\chi} \end{aligned} \quad (4)$$

where a, b, c, d are empirical coefficients determined using Curve Fitting Toolbox in Matlab.

The term for volume air flow was modeled according to equations given in [20]:

$$\dot{V}_{atm} = \begin{cases} P_1 C \sqrt{\frac{T_0}{T_1}} \sqrt{1 - \left(\frac{\frac{P_2}{P_1} - \psi}{1 - \psi} \right)^2}, & \text{if } \frac{P_2}{P_1} > \psi \\ P_1 C \sqrt{\frac{T_0}{T_1}}, & \text{if } \frac{P_2}{P_1} \leq \psi \end{cases} \quad (5)$$

where P_1 is upstream pressure [Pa], P_2 is downstream pressure [Pa], C is sonic conductance [$\text{m}^3\cdot\text{s}^{-1}\cdot\text{Pa}^{-1}$], T_0 is reference temperature [K], T_1 is upstream temperature [K] and ψ is critical ratio.

To derive the dynamics of rotational axis, Lagrangian mechanics approach was used. According to [21] it is possible to write:

$$\frac{d}{dt} \left(\frac{\partial L}{\partial \dot{q}_i} \right) - \frac{\partial L}{\partial q_i} = \tau_i, \text{ where } L = K - P \quad (6)$$

where K is kinetic energy, P is potential energy, q_i is generalized variable, τ_i is generalized force. Since the actuator used a single rotational axis (one degree-of-freedom), generalized variable corresponded to joint (arm) angle β [°]. Furthermore, as only changes in potential energy are relevant and actuator moved in horizontal plane, P was set to zero. Therefore, (when friction is neglected) the following holds:

$$\begin{aligned} q &= [\beta], \dot{q} = [\dot{\beta}], \tau = [T], K = \frac{1}{2} J \dot{\beta}^2 \\ J \ddot{\beta} &= T - T_L, \text{ where } T = (F_1 - F_2)r \end{aligned} \quad (7)$$

where J is moment of inertia [$\text{kg}\cdot\text{m}^2$], T is torque [$\text{N}\cdot\text{m}$], $F_{1,2}$ are muscle forces [N] and r is chainwheel diameter [m].

B. Elman Network for Improved Dynamic Modeling

The model presented in previous paragraph captures the dynamics of PAM-based actuator quite well under nominal conditions. If, however, higher accuracy is required there is a number of effects that might be difficult to describe analytically (static and dynamic hysteresis, structural dynamics etc.). Since the model was intended to be used for model-based design of a hybrid controller (PD-fuzzy), closed-loop performance of derived model was of high importance.

According to [21] a general vector equation for dynamics of n link robot can be expressed in the following form:

$$\begin{aligned} \mathbf{M}(\mathbf{q})\ddot{\mathbf{q}} + \mathbf{N}(\mathbf{q}, \dot{\mathbf{q}}) + \boldsymbol{\tau}_p &= \mathbf{F} \\ \mathbf{N}(\mathbf{q}, \dot{\mathbf{q}}) &\equiv \mathbf{V}(\mathbf{q}, \dot{\mathbf{q}})\dot{\mathbf{q}} + \mathbf{T}(\dot{\mathbf{q}}) + \mathbf{G}(\mathbf{q}) \end{aligned} \quad (8)$$

where \mathbf{q} – generalized variable vector, $\mathbf{M}(\mathbf{q})$ is inertia matrix, $\mathbf{V}(\mathbf{q}, \dot{\mathbf{q}})\dot{\mathbf{q}}$ is Coriolis/centripetal forces term, $\mathbf{T}(\dot{\mathbf{q}})$ is friction forces term, $\mathbf{G}(\mathbf{q})$ is gravity term, \mathbf{F} – generalized force vector and $\boldsymbol{\tau}_p$ is disturbance term.

The equation expressed in (8) reduces to a simple form for our case as only one joint was used and the actuator moved in horizontal plane (term $\mathbf{G}(\mathbf{q})$ was dropped). The aforementioned effects of unmodeled dynamics were incorporated into $\boldsymbol{\tau}_p$ term. Due to the powerful approximation capabilities of neural networks, it is proposed here to use recurrent neural network to identify the disturbance term.

In Fig. 3 the scheme of identification of disturbance term in closed-loop is depicted. In this scheme PAM-based Actuator block corresponds to a complete closed-loop control of actuator using PD controller with β^* being desired joint angle and β_s being actual joint angle. The desired joint angle is also an input into a model of PAM-based actuator output of which is labeled β_m . The difference between actual and model joint angle corresponds to a modeled disturbance term τ_p , which incorporates all the effects not included in analytical model of PAM actuator. This term was to be approximated using neural network so that a disturbance term error e_τ (defined as difference between actual disturbance term τ_p and neural network disturbance term τ_{pnn}) was minimal. Since the complete model was intended for simulation of PAM-based actuator in model-based control system design, the input into the neural network had to be provided by the primary analytical model (labeled as \mathbf{U}_m).

As an approximator, recurrent neural network type with feedback from hidden layer (Elman network) was chosen. This was preferred over external dynamics approach using input dynamic filter and static neural approximator (nonlinear autoregressive model with exogenous input).

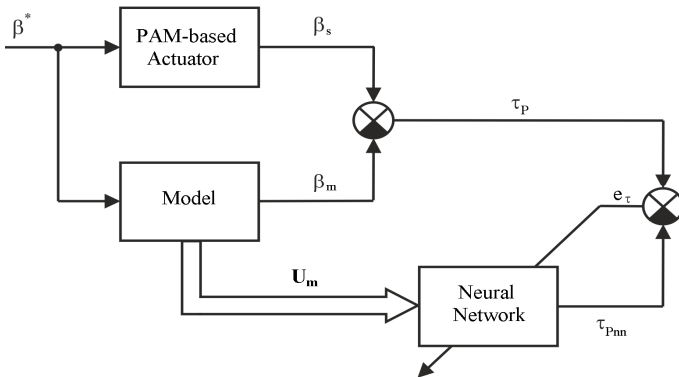


Fig. 3. Identification of disturbance term of PAM-based actuator using neural network

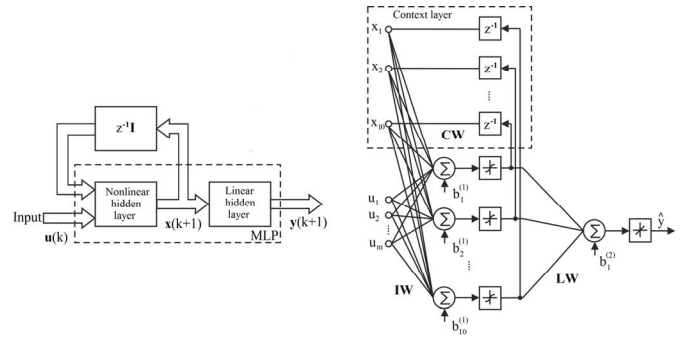


Fig. 4. State diagram of Elman network (left) and its structure for disturbance term identification (right)

This approach was selected due to the relaxed requirement on the knowledge of dynamic order as well as its better suitability for simulation [22]. State equations for Elman network in Fig. 4 can be written as follows:

$$\begin{aligned} \mathbf{x}(k+1) &= \mathbf{f}(\mathbf{C}_w \mathbf{x}(k) + \mathbf{I}_w \mathbf{u}(k) + \mathbf{b}^{(1)}) \\ y(k) &= \mathbf{L}_w \mathbf{x}(k) + \mathbf{b}^{(2)} \end{aligned} \quad (9)$$

where \mathbf{f} is vector of nonlinear (tanh) functions, \mathbf{C}_w is context layer weight matrix, $\mathbf{x}(k)$ is state vector in time step k , \mathbf{I}_w is input layer weight matrix, $\mathbf{u}(k)$ is input vector in time step k , \mathbf{L}_w is hidden layer weight matrix and \mathbf{b} is bias vector. By substituting (9) into (8) we get:

$$\boldsymbol{\tau}_p = \mathbf{L}_w \mathbf{f}(\mathbf{C}_w \mathbf{x}(k) + \mathbf{I}_w \mathbf{u}(k) + \mathbf{b}^{(1)}) + \mathbf{b}^{(2)} + e_\tau \quad (10)$$

where e_τ is approximation error of neural network.

III. RESULTS

Experiments for verification of the proposed approach were carried out in closed-loop for position control with a conventional PD controller. So far only the joint angle was taken into account in improved model validation as this was the main control variable in intended control scheme. The model was validated using the MAE (Mean Absolute Error) criterion defined as follows:

$$MAE = \frac{1}{n} \sum_{k=1}^n |y_k - \hat{y}_k| \quad (11)$$

where k is time step, n is number of samples, y_k is actuator output in k -th time step and \hat{y}_k is model output in k -th time step.

To validate the model, the responses of model and actuator to a sequence of reference joint angle steps (with alternating sign) are compared (Fig. 5 and Fig. 6). This was done for both nominal moment of inertia ($J_n = 0.014 \text{ kg}\cdot\text{m}^2$) and its 6.4 multiple ($J = 6.4 \cdot J_n = 0.0896 \text{ kg}\cdot\text{m}^2$). Good representation of the actuator dynamics for changes in moment of inertia was important for control system design.

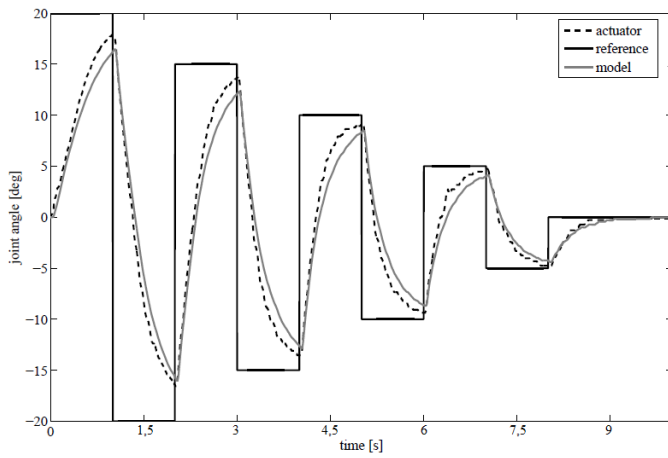


Fig. 5. Model and actuator responses to a sequence of step changes in reference joint angle in closed loop with PD controller for $J = J_n$

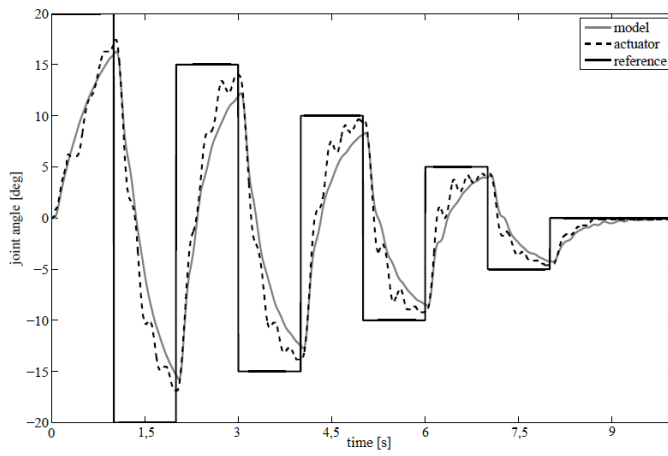


Fig. 6. Model and actuator responses to a sequence of step changes in reference joint angle in closed loop with PD controller for $J = 6.4J_n$

What is readily observable from both figures is the difference in oscillations of responses associated with the change of moment of inertia. This increase in oscillatory nature of responses can be linked to the manifestation of structural dynamics that is not incorporated in the model. Quantitatively, for nominal moment of inertia model error expressed in *MAE* was 1.1708 and for 6.4 multiple *MAE* was 1.2887. The error for nominal case could be decreased by modifying model parameters which would, however, have increased model error for other model variables (the values of these parameters were selected so that the error for all variables that could be measured was minimal). On the other hand, the same approach for non-nominal case did not produce responses with similar oscillations as were measured for real actuator. The effect of structural dynamics thus was not well represented in the model and could be treated as an external disturbance expressed in term τ_p .

To improve the dynamic performance of the model, an Elman network with the structure shown in Fig. 4 was used. The number of neurons was set to $N = 10$ which was the upper limit for using an enhanced training algorithm with much shorter training times [23]. For training, Levenberg-Marquardt algorithm with Bayesian regularization was utilized.

As was mentioned in previous paragraph, the input into Elman network (U_m) was provided from the analytical model. The best results were obtained for five variables in U_m : reference angle, PD control signal, joint angle, joint angular velocity and joint angular acceleration. In order to obtain good representation of underlying nonlinear function in terms of experimental data used for training, it was necessary to excite the actuator as richly as possible. Due to this reason, APRBS (Amplitude Pseudo-Random Binary Sequence) signal was chosen consisting of steps with random height and width within the range of $[-40^\circ, 40^\circ]$ (Fig. 7 grey line). Using the difference between measured and modeled joint angle for $J = 6.4J_n$, an error signal was produced and used as a target sequence (actually τ_p) for Elman network (Fig. 7 black line).

The sampling period used in simulation as well as during the measurements and control was set to 3 ms. Thus the number of samples in 200 s sequence was 66667. This sequence of samples was used as a training set while 3334 samples used as an excitation signal in Fig. 5 and Fig. 6 were used as a test set (this sequence was not used during the training). The validation set was not used due to the utilization of Bayesian regularization (instead of early stopping method).

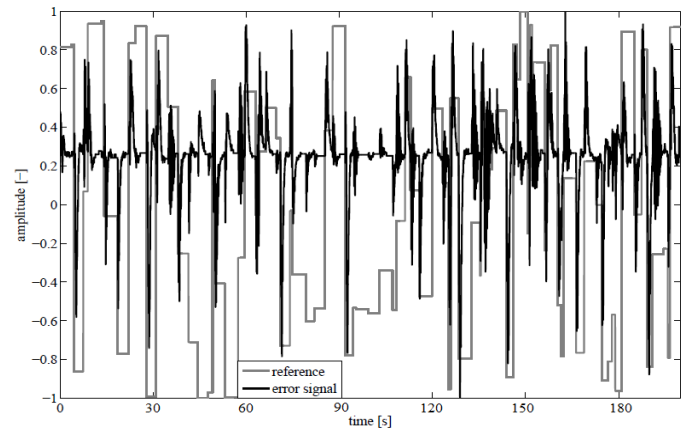


Fig. 7. Amplitude pseudo-random binary sequence (APRBS) signal used for actuator excitation and error signal used for supervised network training (the amplitude of both signals was normalized into $[-1, 1]$ interval)

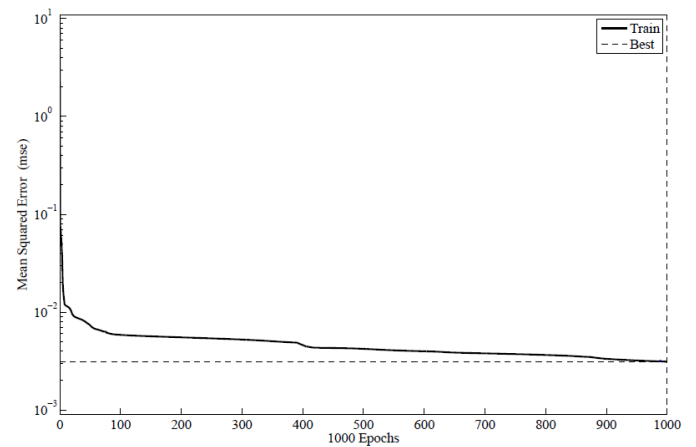


Fig. 8. The training plot (first 1000 iterations) for Elman network training

The progress of training for the first 1000 iterations is shown in Fig. 8 with the results of training after 5000 iterations being shown in Table I.

TABLE I. NETWORK TRAINING RESULTS

iter	time	MSE	grad	μ	γ
5000	36101	0.0015	1.43	5×10^5	156

It is of note that the resulting MSE (0.0015) applies to signals normalized into $[-1,1]$ range. This can be considered a good result as this translates to 0.075% mean relative error (when the whole normalized range is taken into account). In Tab. I the symbols μ and γ denote Levenberg-Marquardt algorithm conditioning (or damping) factor and number of effective parameters respectively.

Limiting value for μ was set to 10^{10} which was not reached during the training implying that the extremum might not have been attained. Nevertheless, the decrease in MSE in the last 1000 iterations was very slow and thus the minimum of error function was not possibly very much different from the obtained value. The final value for γ (which means the number of network parameters effectively used for decreasing the error function [24]) was relatively close to the number of all parameters of the network (equal to 171). In that case the number of neurons should be increased to test whether the original network is capable of sufficiently represent the underlying function. As the final MSE was considered good enough and increasing the number of neurons would lead to very long training times (due to the training without enhanced training algorithm), this method was not yet tested.

In Fig. 9 the results of validation of neurally enhanced analytical model are shown. The test was carried out using the alternating step sequence for reference joint angle (3334 samples). It can be observed that compared to Fig. 6 the model now also captures oscillating character of the response for increased moment of inertia. Higher discrepancy between the model and the actuator can be seen in the beginning which can be possibly attributed to zero network initialization.

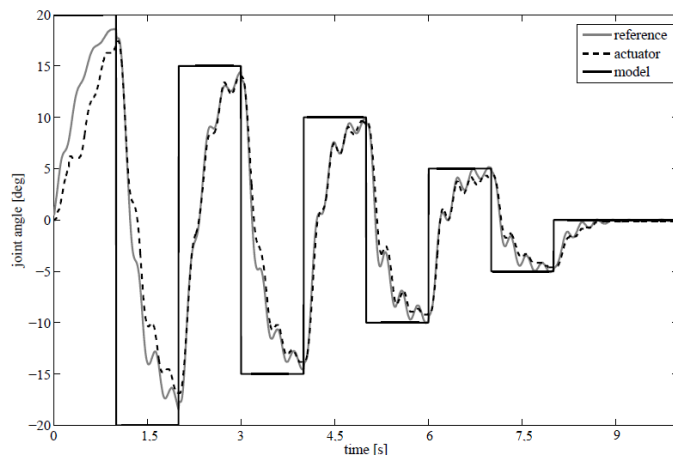


Fig. 9. Validation of neurally enhanced model performance on test data for $J = 6.4J_n$

The accuracy is quickly improved from the second positive reference angle step on. The value of MAE criterion for the response shown in Fig. 9 was decreased from 1.2887 to 0.9793 which is almost exactly 24% improvement in the mean absolute error. It is assumed that it would be possible to decrease MAE by further modifications of the neural model. More precisely, three possible factors can be considered for improving the accuracy of neurally enhanced model: increasing the richness of excitation signal (hence increasing the size of training data set), modifying or enlarging network input vector U_m and increasing the number of neurons. The last two of these approaches are currently prevented by the impossibility to use enhanced training algorithm.

IV. CONCLUSION

In this paper we presented an enhancement of analytical dynamic model of one-DOF pneumatic muscle actuator using the recurrent neural network. It was shown that while the basic actuator dynamics is captured by the original analytical model, it failed to account for most of the effects associated with hard-to-model phenomena present in PAM-based actuators (as well as the specific actuator construction). Neural networks as universal approximators have powerful approximation capabilities and they are thus suitable for identifying such complex phenomena. To preserve the physical interpretation of the model, it was proposed here to use neural network only to identify unmodeled dynamics treated as an external disturbance. Recurrent neural network was preferred over more usual NARX model with input filter due to the better long-term prediction capabilities. It was shown that such an approach is viable solution for improving the accuracy of PAM-based system model. Even though this approach was presented only for joint angle modeling enhancement, it is assumed that it is equally well suitable for modeling enhancement of other system variables provided that relevant training data are available. In further work, we assume to extend the approach to model enhancement for different changes in moment of inertia as well as to increase its accuracy.

ACKNOWLEDGMENT

The research work is supported by the Project of the Structural Funds of the EU, title of the project: Research and development of intelligent nonconventional actuators based on artificial muscles, ITMS code: 26220220103.

REFERENCES

- [1] K. Židek and J. Šeminský, "Automated rehabilitation device based on artificial muscles", *Annals of DAAAM for 2011 & Proceedings of the 22nd International DAAAM Symposium*, 23-26th November 2011, Vienna: DAAAM, pp. 1113-1114.
- [2] K. Židek, J. Piteľ, A. Galajdová and M. Fodor, "Rehabilitation device construction based on artificial muscle actuators", *Proceedings of the Ninth IASTED International Conference: Biomedical Engineering BioMed 2012*, February 15-17, 2012, Innsbruck: ACTA Press, pp. 855-861.
- [3] K. Židek, O. Liška and V. Maxim, "Rehabilitation device based on unconventional actuator", *Mechatronics: Recent Technological and Scientific Advances*, R. Jablonski and T. Březina, Eds., Berlin: Springer-Verlag Berlin Heidelberg, 2011, pp. 697-702.

- [4] M. Tóthová, J. Pitel' and J. Mižáková, "Electro-pneumatic robot actuator with artificial muscles and state feedback", *Applied Mechanics and Materials*, 2014, vol. 460 (2014), pp. 81-90.
- [5] M. Balara, "The upgrade methods of the pneumatic actuator operation ability", *Applied Mechanics and Materials*, 2013, vol. 308 (2013), pp. 63-68.
- [6] M. Balara and A. Vagaská, "The torque moment of rotary actuator with artificial muscles", *Proceedings of ARTEP 2013*, February 20-22, 2013, Košice: TU, pp. 31-1 – 10.
- [7] J. Boržiková, J. Pitel', M. Tóthová and B. Šulc, "Dynamic simulation model of PAM based antagonistic actuator", *Proceedings of the 2011 12th International Carpathian Control Conference (ICCC)*, 25–28th May 2011, Ostrava: IEEE, pp. 32–35.
- [8] M. Balara and M. Tóthová, "Static and dynamic properties of the pneumatic actuator with artificial muscles", *Proceedings of the IEEE 10th Jubilee International Symposium on Intelligent Systems and Informatics (SISY 2012)*, September 20-22, 2012, Subotica: IEEE, pp. 577-581.
- [9] A. Macurová and S. Hrehová, "Some properties of the pneumatic artificial muscle expressed by the nonlinear differential equation", *Advanced Materials Research*, 2013, vol. 658 (2013), pp. 376-379.
- [10] M. Tóthová, J. Pitel' and J. Boržiková, "Operating modes of pneumatic artificial muscle actuator", *Applied Mechanics and Materials*, 2013, vol. 308 (2013), pp 39-44.
- [11] A. Vagaská, Mathematical description and static characteristics of the spring actuator with pneumatic artificial muscle, *Applied Mechanics and Materials*, 2014, vol. 460 (2014), pp. 65–72.
- [12] S. Davis, N. Tsagarakis, J. Canderle and D. G. Caldwell, "Enhanced modelling and performance in braided pneumatic muscle actuators", *International Journal of Robotics Research*, 2003, vol. 22, no.3-4, pp. 213-227.
- [13] S. Davis and D. G. Caldwell, "Braid effects on contractile range and friction modelling in pneumatic muscle actuators", *International Journal of Robotics Research*, 2006, vol. 25, no. 4, pp. 359-369.
- [14] T. Kerscher, J. Albiez, J. M. Zollner and R. Dillmann, "Evaluation of the dynamic model of fluidic muscles using quick-release", *Proceedings of the 1st IEEE/RAS-EMBS International Conference on Biomedical Robots and Biomechatronics*, 20-22 February, 2006, Pisa: IEEE, pp. 637-642.
- [15] P. B. Petrovič, "Modeling and control of an artificial muscle", *The Xth Conference on Mechanical Vibration (CVM 2002)*, May 23-24, 2002, Timisoara: Universitatii Politehnica, 2002, pp. 93-106.
- [16] J. L. Serres, "Dynamic characterization of a pneumatic muscle actuator and its application to a resistive training device", thesis, Dayton, Ohio: Wright State University, 2008.
- [17] A. Hošovský and M. Havran, "Dynamic modeling of one-degree-of-freedom pneumatic muscle - based actuator for industrial applications", *Tehnicki Vjesnik*, 2012, vol. 19, no. 3, pp.673-681.
- [18] M. Tóthová and A. Hošovský, "Dynamic simulation model of pneumatic actuator with artificial muscle", *Proceedings of the IEEE 11th International Symposium on Applied Machine Intelligence and Informatics (SAMI 2013)*, January 31 - February 2, 2013, Herl'any, Košice: IEEE, pp. 47-51.
- [19] J. Pitel' and M. Tóthová, "Dynamic modeling of PAM based actuator using modified Hill's muscle model", *Proceedings of the 2013 14th International Carpathian Control Conference (ICCC)*, 26 – 29 May 2013, Rytro, Kraków: IEEE, 2013, pp. 307-310.
- [20] P. Beater, "Pneumatic Drives: System design, modelling and control", New York: Springer Verlag, 2007.
- [21] F. L. Lewis, D. M. Dawson and C. T. Abdallah, "Robot Manipulator Control", New York: Marcel Dekker, Inc., 2004.
- [22] O. Nelles, "Nonlinear system identification: from classical approaches to neural networks and fuzzy models", Berlin: Springer Verlag, 2001.
- [23] <http://www.mathworks.com/help/releases/R2012b/nnet/release-notes.html>
- [24] F. D. Foresee and M. T. Hagan, "Gauss-Newton approximation to Bayesian Learning", *Proceedings of the International Conference on Neural Networks*, 9-12 June, 1997, Houston: IEEE, pp. 1930-1935.